IJITCE

ISSN 2347- 3657

International Journal of Information Technology & Computer Engineering

Email : ijitce.editor@gmail.com or editor@ijitce.com

International Journal of Information Technology & Computer Engineering

ISSN 2347–3657

Volume 12, Issue 2, 2024

Innovative High Step-Up Soft Switching Interleaved DC-DC Boost Converter with Coupled Inductors for Photovoltaic Applications

Maddali Supriya[1],Sri Harsha Giri[1] , Abdul Razak[2], Karre Vamsi[2], Kona Sai Sumanth[2], Kodali Manasa[2]

[1]Assistant Professor, Department of Electrical and Electronics Engineering, SRK Institute of Technology-Enikepadu, Vijayawada-521108, Andhra Pradesh, India

[2]Department of Electrical and Electronics Engineering, SRK Institute of Technology-Enikepadu, Vijayawada-521108, Andhra Pradesh, India

SSABSTRACT:

"This study introduces an innovative design for a high-step-up DC-DC converter suitable for decentralized power systems. The design employs a unique combination of two capacitors and a single coupled inductor. During the off-state of the switch, the stored energy in the coupled inductor charges the capacitors in parallel, and during the on-state, discharges them in series, achieving a high step-up voltage gain. Additionally, a passive clamp circuit recycles the energy lost due to the leakage inductance of the coupled inductor, thereby reducing the voltage stress on the primary switch. Utilizing a switch with low on-resistance reduces conduction losses significantly. Moreover, enhancements in diode reverse-recovery issues further improve efficiency. The paper provides detailed discussions on the operational principles and steady-state analyses of the converter."

1. INTRODUCTION:

When the world's population grows, so does its need for energy, and as traditional sources run dry, it is imperative that alternative forms of power be developed to meet rising demand. A larger population is to blame for the rise in electrical use. As a result, several power plants have been built around the nation to keep up with the demand. Two distinct methods are being used to create energy. The grid transports the electricity produced by these facilities to the end user. Electricity is crucial to the growth of industry and, more broadly, to society. Using a geyser, heater, toaster, etc., are all common examples of daily electrical appliances. Power production and transmission must be scaled up to satisfy consumer demand at a reasonable cost. The versatility of electrical energy makes it ideal for both home and commercial use (i.e., lighting, mechanical work). One of the most accurate measures of a country's level of development is its per capita usage of electricity. Possession of a vehicle, a mobile phone, or a home would be further signs.

Fossil fuels (coal, oil, and natural gas), as well as nuclear and hydro resources, are converted into conventional sources. Coal, oil, and natural gas may all be burned to provide heat energy, which can then be transformed to

mechanical energy and finally electrical energy. By 2020, conventional energy will account for 80% of global power production, while renewable sources will account for just 20%. In a thermo cycler, the heat energy produced by burning fossil fuel (or fission of nuclear material) is transformed into mechanical form, and subsequently the mechanical energy is transferred to electrical energy in generators. There is a dismal lack of heat transfer (40%)[2]. Fewer options exist when using traditional methods. Coal burning must be reduced, minimised, or somehow conserved, thus we must turn to other energy sources, such as renewable, green, or natural energy, while keeping environmental and financial concerns in mind. As the global population grows rapidly, so does the need for energy, and scientists and engineers have predicted that we will soon exhaust the Earth's nonrenewable fuel supplies.

2. DC-DC CONVERTERS:

A device that is used in order to alter the level of DC voltage is known as a direct current (DC) to direct current (DC) converter. It is possible for the voltage to move in either direction, from low to high or high to low. It was common practise, before to the development of power semiconductors and other associated technologies, to enhance the DC supply voltage for low-power applications by combining the functions of a rectifier, a step-up transformer, and a vibrator.

An electric motor was coupled to a generator set operating at the necessary voltage in order to boost the available power (sometimes combined into a single "dynamotor" unit). People would only turn to these inefficient and pricey techniques if they were forced to, for example, power a vehicle radio (which, back then, used thermionic valves/tubes that required considerably greater voltages than are available from a 6 or 12 V car battery).

These techniques, which include converting a direct current (DC) power source to an alternating current (AC), then using a transformer to modify the voltage (which is tiny, light, and inexpensive because of the AC), and lastly rectifying back to DC, became economically feasible with the development of power semiconductors and integrated circuits. Other techniques include converting alternating current (AC) into direct current (DC). Even when transistorised power supplies were available, some amateur radio operators continued to utilise vibrator supplies and dynamotors for mobile transceivers that required high voltages. A dynamotor is a motor and generator integrated into a single device, with one winding operating the motor and the other winding creating the output voltage. [15]

3. PROPOSED CONVERTER

The core of the maximum power point tracking hardware is the DC-DC converter that is shown in Figure 4. It adheres to the MPP and guarantees the DC link voltage even in areas with low levels of illumination. The majority of DC/DC converters, including buck, boost, buck-boost, cuk, sepic, and zeta converters, among others, are often run at high switching frequencies, which results in a rise in switching losses, noises, and component stresses. Because of these problems, the performance of the standard boost converter deteriorates, which leads to a decrease in the amount of power that is generated. As a potential solution to the problems described above, the authors of the

ISSN 2347–3657

Volume 12, Issue 2, 2024

study recommended a modified interleaved boost converter with twin inductors and a voltage multiplier. This configuration would enable high-step-up applications while minimising the input current ripple.

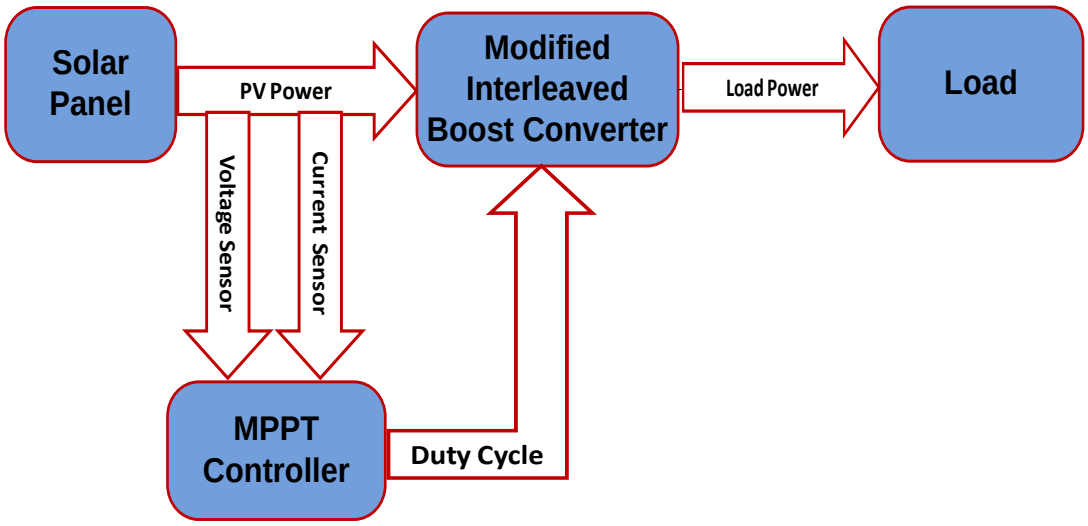

Fig 4.4: Block diagram of Proposed DC/DC conversion

3.1 Principle of operation of SSIBC:

A schematic representation of the proposed network design may be seen in the figure. The related circuit and gate control schematics for the SSIBC of two single-phase boost inverters linked in parallel and inverters running 180 degrees out of phase with 30 kHz switching frequency are shown in figures 4.5 and 4.6, respectively.

A modified interleaved boost converter is the first component of a two-part circuit that also contains a voltage multiplier. The voltage multiplier is the second component of the circuit.

The modified Interleaved boost control serves two primary purposes: (i) reduced output ripple from series-connected capacitor interleaving, and (ii) reduced switch voltage stress.

International Journal of Information Technology & Computer Engineering

ISSN 2347–3657

Volume 12, Issue 2, 2024

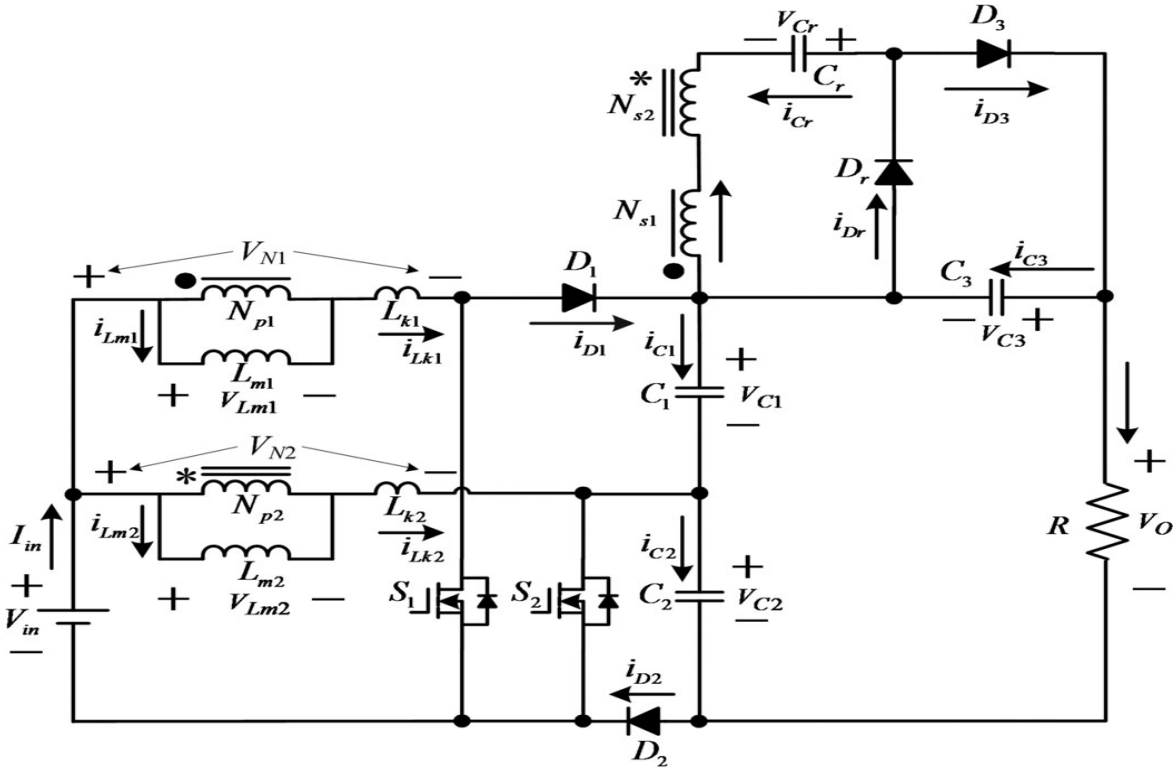

Fig4.5: Circuit diagram of SSIBC

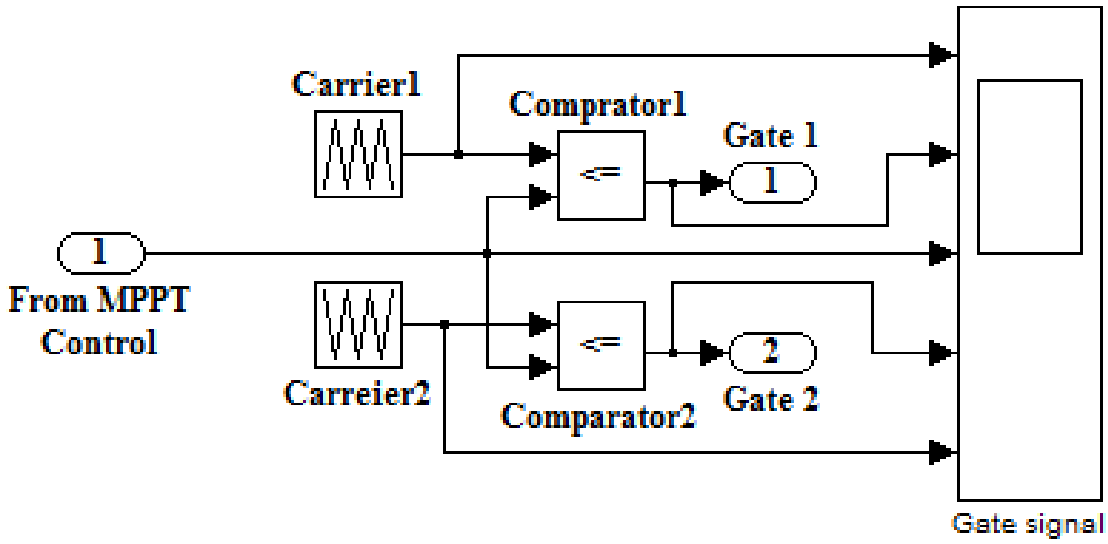

Fig4.6: Gate control signal

The operating stages can be explained as follows:

International Journal of Information Technology & Computer Engineering

ISSN 2347–3657

Volume 12, Issue 2, 2024

First stage *($t_0 - t_1$):*-Leakage Inductance Lk1 causes Power Switch S1 to turn ON with ZCS at time t=, while S2 remains ON and all diodes are OFF save for D3. This is depicted in Fig 4.10. Leakage Inductances allow for fine-grained regulation of the current decaying through D3, greatly reducing the impact of the reverse recovery problem. Leakage inductances LK1 and LK2 and magnetising inductances LM1 and LM2 are charged linearly by an input voltage source Vin.

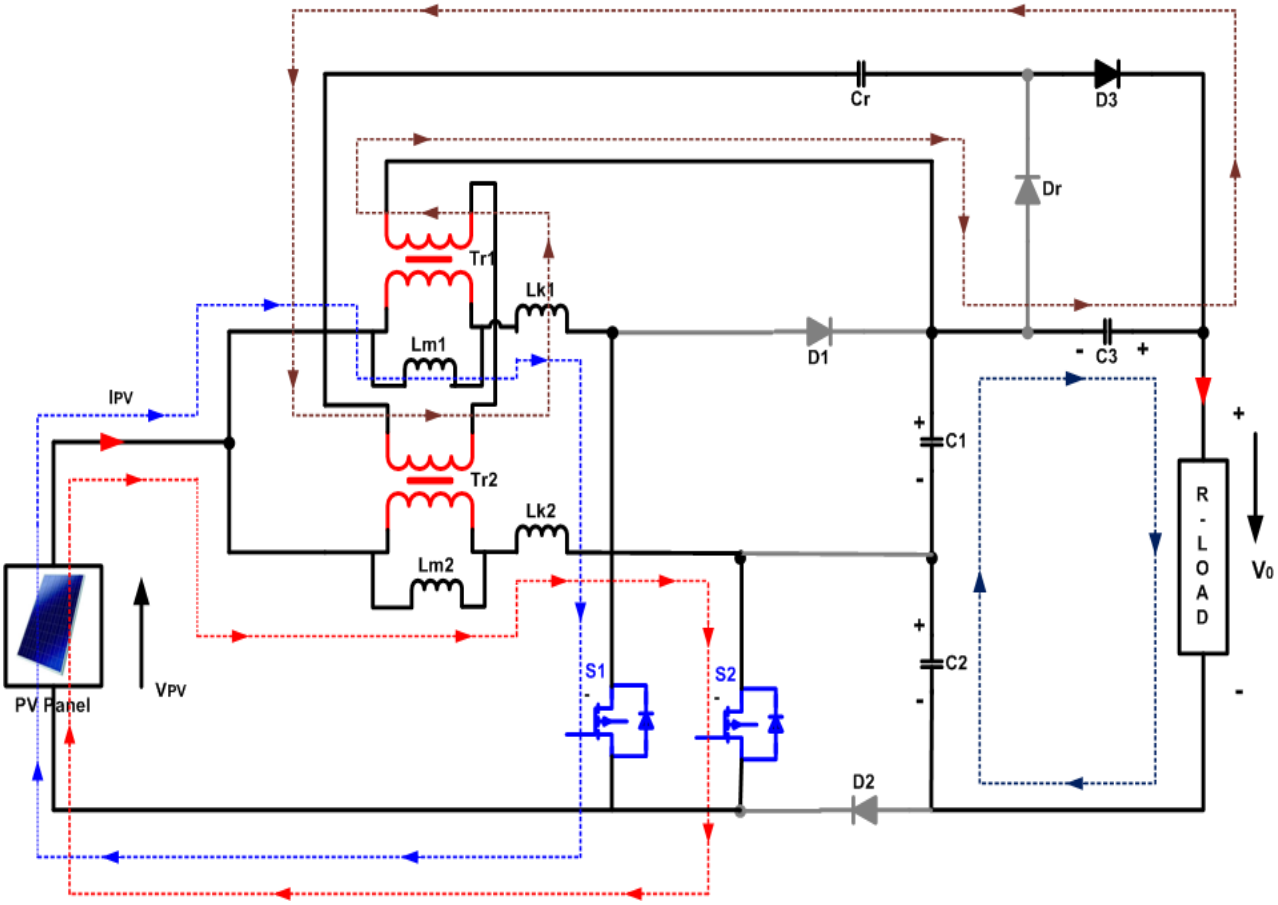

Second stage *($t_1 - t_2$):*-At t=t1 switch S2 is turn OFF, diodes D2 and Dr turn ON. The input voltage source, magnetising Inductances LK2 discharges the energy to C2 through diode D2 as shown in Fig 4.11. Even after the leakage inductance, LK2, has discharged all of its energy to the capacitor, the magnetising inductance, LM2, continues to discharge energy to the secondary side, charging the capacitor, Cr, through the diode, Dr.

International Journal of Information Technology & Computer Engineering

ISSN 2347–3657

Volume 12, Issue 2, 2024

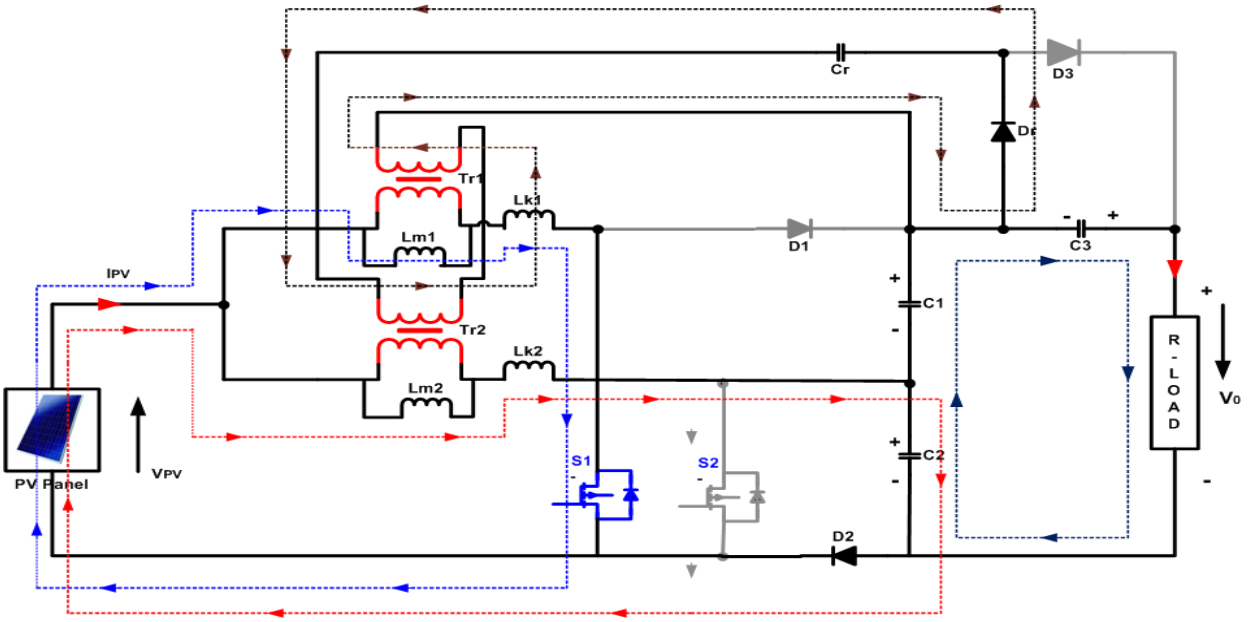

Third stage ***($t_2 - t_3$):-***A t= t2 switch With the ZCS condition, S2 is activated. As may be seen in Fig 4.12, S1 does not cycle off. Diode reverse recovery is reduced thanks to LK1 and LK2's regulation of the current via Dr.

Fourth stage ***($t_3 - t_4$):-***Indicated by the symbol t=, this switch As shown in Fig. 4.13, when S1 is turned OFF and S2 is left in its conducting state (ON state), energy from V PV, Lm1, and Lk1 is transferred to C1 through S2. The Lm1 capacitor releases its stored energy to the secondary side of the transformer. Second-side current is routed in series to C3 and then to the load via D3.

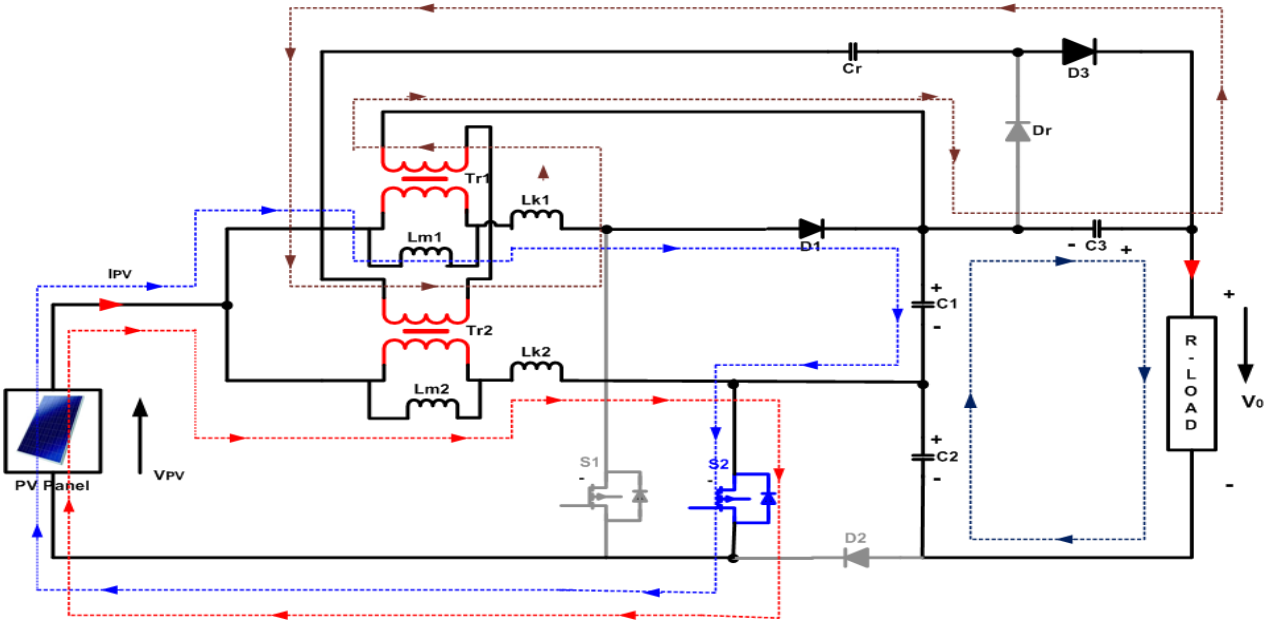

International Journal of Information Technology & Computer Engineering

ISSN 2347–3657

Volume 12, Issue 2, 2024

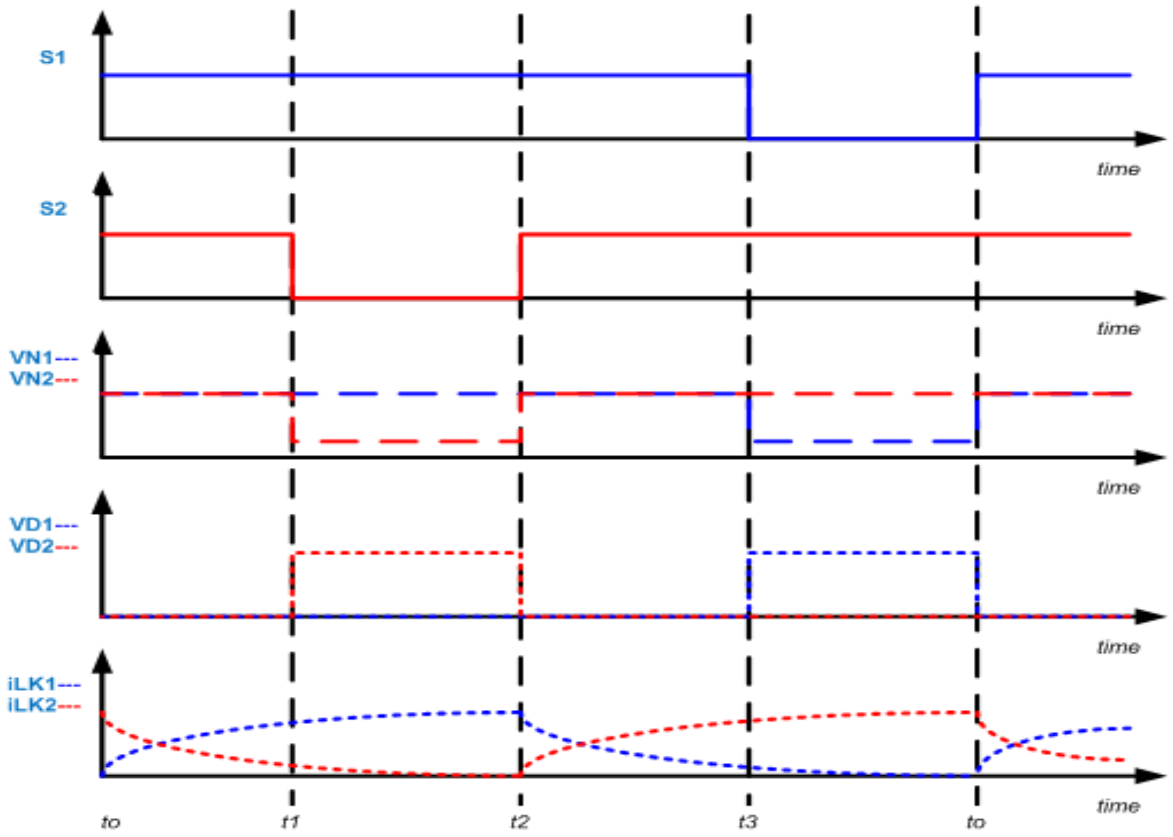

Figure Switching sequence of proposed SSIBC

Voltage Gain Expression

At stage second

$$V_0 = V_{c1} + V_{c2} + V_{c3} \quad (4.1)$$

At stage three

$$V_{cr} = V_{s1} - V_{s2} = KNV_{c2} \quad (4.2)$$

$$V_{c3} = V_{cr} + V_{s2} - V_{s1} = KN(V_{c1} + V_{c2}) \quad (4.3)$$

Voltage across the capacitors $C_1$and C_2 are obtained as

$$V_{c1} = V_{c2} = \frac{V_{in}}{1-D} \quad (4.4)$$

Voltage across the capacitors $C_3$and C_r are obtained as

$$V_{c3} = \frac{2KN}{1-D} V_{in} \quad (4.5)$$

$$V_{cr} = \frac{KN}{1-D} V_{in} \quad (4.6)$$

Substituting (4) and (5) in (1) to obtain output voltage

$$V_0 = \frac{V_{in}}{1-D} + \frac{V_{in}}{1-D} + \frac{2KN}{1-D} V_{in} \quad (4.7)$$

The ratio of the voltage at the output terminal to the voltage at the input terminal is the formula for calculating voltage gain.

$$\frac{V_0}{V_{in}} = \frac{2}{1-D}(1+KN) \quad (4.8)$$

If one does not take into account the influence of leakage inductances, the coefficient of coupling is equal to 1. The voltage gain is recalculated after that as

$$\frac{V_0}{V_{in}} = \frac{2(1+N)}{1-D} \quad (4.9)$$

The source of the voltage strain that is placed on the power switches S1 and S2 is

$$V_{s1-stress} = V_{s2-stress} = \frac{V_{in}}{1-D} = \frac{V_0}{2(1+N)} \quad (4.10)$$

The voltage stress on the diodes D_1, D_2, D_3 and D_r related to the turns ratio and the output voltage can be derived as

$$V_{D1-stress} = \frac{2V_{in}}{1-D} = \frac{V_0}{(1+N)} \quad (4.11)$$

$$V_{D2-stress} = \frac{V_{in}}{1-D} = \frac{V_0}{2(1+N)} \quad (4.12)$$

$$V_{D3-stress} = V_{Dr-stress} = \frac{2NV_{in}}{1-D} = \frac{NV_0}{(1+N)} \quad (4.13)$$

In this configuration, a voltage multiplier is placed across the output of two classical boost converters that are linked in parallel with a pair of dual-coupled inductors. When switch S1 is in the on position, the input voltage flows through the inductors, charging them. When S2 is on, the voltage multiplier is connected across the circuit and the inductors are discharged. Leakage Inductance Lk1 causes ZCS to activate switch S1, keeping S2 in its on position and all diodes off with the exception of D3. Leakage Inductances allow for fine-grained regulation of the current decaying via D3, greatly reducing the impact of the reverse recovery issue. Leakage inductances LK1 and LK2 and magnetising inductances LM1 and LM2 are charged linearly by an input voltage source Vin.

When time (t=t1) is reached, diodes D2 and Dr are activated by turning off switch S2. Diode D2 transfers energy from the input voltage source via the magnetising inductances LK2 and then onto capacitor C2. Even after the leakage inductance, LK2, has discharged all of its energy to the capacitor, the magnetising inductance, LM2, continues to discharge energy to the secondary side, charging the capacitor, Cr, through the diode, Dr.

The ZCS condition activates the t= t2t 3 switch S2. To this day, S1 has not been toggled off. Diode reverse recovery is reduced thanks to LK1 and LK2's regulation of the current via Dr.

4. SIMULATION RESULTS:

The simulation results validated the performance features of the proposed SSIVB converter. The performance of the suggested converter was simulated and analysed using MATLAB/SIMULINK. The simulation findings were used to inform the construction of a 500VA prototype of the planned SSIVB converter, which was addressed in detail in section 4.5. The circuit parameters and components used are listed in Table 1.

Table 1: Specifications of Proposed Converter

Parameter	Value
Power Rating	500 VA
Input Voltage	36 V
Output Voltage	160 V
Magnetizing Inductance (L_m)	120µH
Leakage Inductance (L_k)	2.1µH
Clamp Capacitors (C_1& C_2)	220µF
Clamp Capacitor (C_3)	470µF
Regenerative Capacitor (Cr)	47µF
Turns Ratio of transformer	1.055

4.6.1 Simulation Results with INC-MPPT Method

The simulation results for suggested converter are presented in figure 4.15. In this section suggested converter is linked between the STH-250WH PV source and load resistance. Gate signal in a converter is created from INC-MPPT system by considering the duty cycle.

For the simulation, the varying irradiance values given in Fig 4.15 (500 W/m2 from 0 to 1 sec, 1000 W/m2 from 1 to 2 sec, 800 W/m2 from 2 to 3 sec, and 600 W/m2 from 3 to 4 sec) are taken into account (i). Input and output voltage of the proposed converter are presented in figure 4.15 (ii) & (iii) (iii)

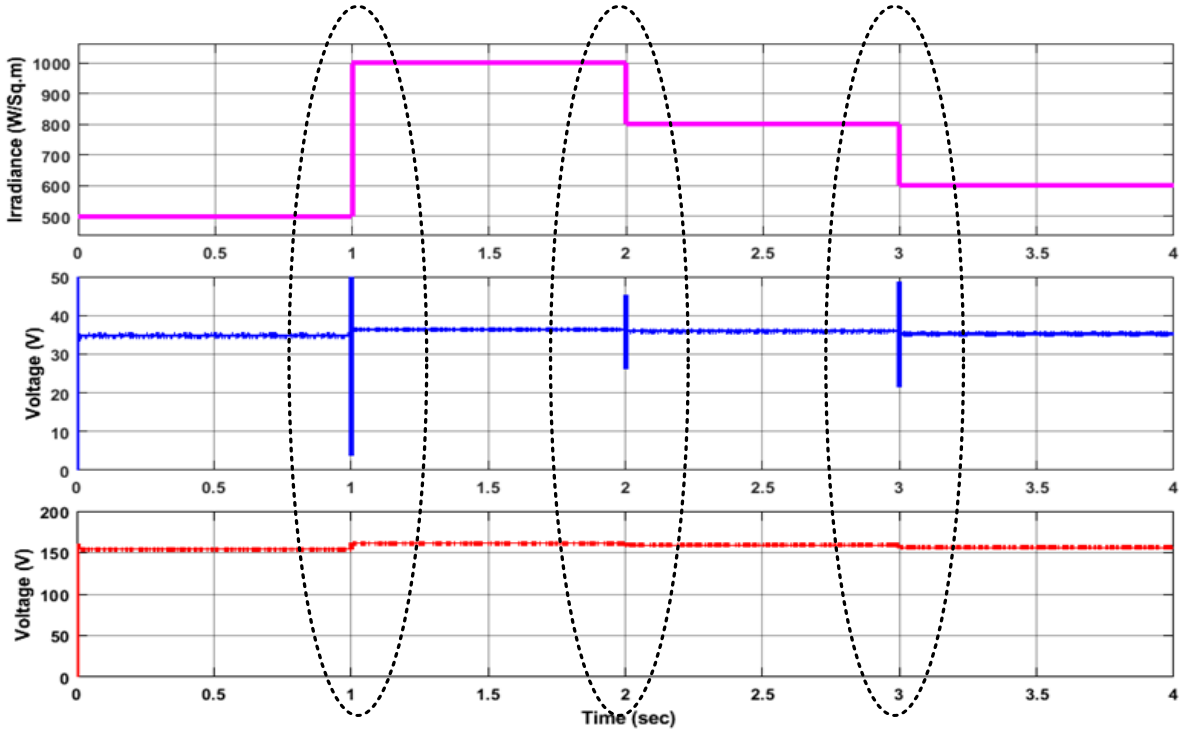

Figure 4.15: Simulation results of the proposed converter with INC-MPPT for the irradiance variation: (i) Irradiance; (ii) Input voltage of the converter; (iii) Output voltage of the converter

When the timer is set to zero, the PV system's output voltage is increased from thirty-five volts to one hundred and thirty-five volts, with a power density of five hundred watts per square meter. There is a 4.25 percent benefit under these circumstances. In Fig 4.15, we see that when the irradiance is raised to 1000 W/m2 at t=1 sec, the PV system's input voltage is 36 V, and the output voltage is raised to 160 V, for a voltage gain of 4.44. At the same time (t = 3 sec), the system is operating at 800 W/m2 and 600 W/m2 input voltage, with an output voltage of around 155 V and a voltage gain of 4.25. Table 2 shows the input voltage, output voltage, and voltage gain for each irradiance level.

Table 2Input and Output Voltages at different irradiance conditions with proposed Method

Time Period(in sec)	Irradiance (in W/m^2)	V_{in} (V)	V_o (V)	Voltage Gain
0 – 1	500	35	153	4.25
1 – 2	1000	36	160	4.44
2 – 3	800	35.6	155	4.25
3 – 4	600	35	155	4.25

CONCLUSION:

So, at the end, the properties of PV module under varying degrees of irradiance and temperature are analysed. The updated MPPT control boosts the tracking efficiency and decreases power loss in PV systems, especially in dynamic conditions. The SSIBC is now ready to be used as an interface for photovoltaic (PV) cells, allowing for the conversion of low voltage input to high voltage output. Reduced voltage stress, quicker transient response to changing irradiance, reduced input current ripple, excellent efficiency, and enhanced dependability are only some of the benefits of the proposed MPPT algorithm over its traditional counterpart.

References:

[1] A. Belkaid, I. Colak, and O. Isik Photovoltaic maximum power point tracking under fast varying of solar radiation, Elsevier ,Applied Energy 179(2016) 523-530.

[2] G.Mamatha, Perturb and Observe MPPT Algorithm Implementation for PV Applications, International Journal of Computer Science and Information Technologies, Vol. 6 (2), 2015, 1884-1887.

[3] Tey Kok Soon, Mekhilef Saad. Modified incremental conductance MPPT algorithm to mitigate inaccurate responses under fast-changing solar irradiation level. Sol Energy 2014;101:333–42.

[4] Houssamo I, Locment F, Sechilariu M. Maximum power tracking for photovoltaic power system: development and experimental comparison of two algorithms. Renew Energy 2010;35:2381–7.

[5] Yu GJ, Jung YS, Choi JY, Kim GS. A novel two-mode MPPT control algorithm based on comparative study of existing algorithms. Sol Energy 2004;76:455–63.

[6] Petreus D, Moga D, Rusu A, Patarau T, Daraban S. A Maximum Power Point tracker for photovoltaic system under changing luminosity conditions. In: IEEE international symposium industrial electronics. ISIE; 2010. p. 556–61

[7] Femia N, Petrone G, Spagnuolo G, Vitelli M. Optimizing sampling rate of P&O MPPT technique. In: Proc. IEEE PESC. p. 1945–9.

[8] A. Reatti, “Low-cost high power-density electronic ballast for automotive HID lamp,” IEEE Trans. Power Electron., vol. 15, no. 2, pp. 361–368, Mar. 2000.

[9] A. I. Bratcu, I.Munteanu, S. Bacha, D. Picault, and B. Raison, “Cascaded DC-DC converter photovoltaic systems: Power optimization issues,” IEEE Trans. Ind. Electron., vol. 58, no. 2, pp. 403–411, Feb. 2011.

[10] H. Tao, J. L. Duarte, and M. A. M. Hendrix, “Line-interactive UPS using a fuel cell as the primary source,” IEEE Trans. Ind. Electron., vol. 55, no. 8, pp. 3012–3021, Aug. 2008.

[11] Y. P. Hsieh, J. F. Chen, T. J. Liang, and L. S. Yang, “Novel high step-up DC-DC converter for distributed generation system,” IEEE Trans. Ind. Electron., vol. 60, no. 4, pp. 1473–1482, Apr. 2013.

[12] M. H. Todorovic, L. Palma, and P. N. Enjeti, “Design of a wide input range dc–dc converter with a robust power control scheme suitable for fuel cell power conversion,” IEEE Trans. Ind. Electron., vol. 55, no. 3, pp. 1247–1255, Mar. 2008.